Available online at www.sciencedirect.com

ScienceDirect

IFAC PapersOnLine 51-34 (2019) 83–88

# Gesture based Human-Swarm Interactions for Formation Control using interpreters

**Aamodh Suresh Sonia Martínez**

*Department of Mechanical and Aerospace Engineering, University of California at San Diego, La Jolla, CA 92093, USA (e-mail: aasuresh@eng.ucsd.edu , soniamd@eng.ucsd.edu)*

**Abstract:** We propose a novel Human-Swarm Interaction (HSI) framework which enables the user to control a swarm's shape and formation. The user commands the swarm utilizing just arm gestures and motions which are recorded by an off-the-shelf wearable armband. We propose a novel interpreter system, which acts as an intermediary between the user and the swarm to simplify the user's role in the interaction. The interpreter takes high level input drawn using gestures by the user, and translates it into low level swarm control commands. This interpreter employs machine learning, Kalman filtering and optimal control techniques to translate the user input into swarm control parameters. A notion of Human Interpretable dynamics is introduced, which is used by the interpreter for planning as well as to provide feedback to the user. The dynamics of the swarm are controlled using a novel decentralized formation controller based on distributed linear iterations and dynamic average consensus. The framework is demonstrated theoretically as well as experimentally in a 2D environment, with a human controlling a swarm of simulated robots in real time.



*Keywords:* Human-Swarm Interaction, Distributed Control, Dynamic Average Consensus, Formation Control, Human Interpretable Dynamics, Gesture Decoding, Hidden Markov Models, Kalman Filter.

## 1. INTRODUCTION

*Motivation.* Due to recent advances in technology, the field of swarm robotics has become pervasive in the research community while slowly permeating to the industry. Although the coordination of multiple robots such as foraging, coverage, and flocking(Olfati-Saber et al., 2006; Jadbabaie et al., 2003; Bullo et al., 2009) has received much attention, the human interaction with robotic swarms is less understood (Kolling et al., 2016). Thus, according to the latest Robotics Roadmap [1] a top priority in swarm robotics is the development of unifying HSI frameworks, the elucidation of rich set of HSI examples, and their comparison. In particular, there is a need to develop novel intuitive interfaces for humans to communicate their intentions to swarms and make it easier for humans to interpret swarms. At the same time, a swarm may require high dimensional and complex control inputs which cannot be intuitively given by a human. Motivated by this, we propose to build a novel supervisory interpreter (Figure 1) to bridge the human and the swarm, which is essential to ensure the effectiveness of a HSI system. We consider the particular problem of formation control, where the human can intuitively draw shapes in the air with his/her arm, which is translated into an effective distributed controller.

*Related Work.* According to recent surveys on HSI (Kolling et al., 2016) and human multi-agent systems (Franchi, 2017), humans either take a supervisory (Savla and Frazzoli, 2012), direct (Setter et al., 2015), shared (Franchi et al., 2012) or environmental (Wang and Schwager, 2016) control role in an HSI framework. Our architecture however, allows humans to provide high level supervisory inputs that are also direct and detailed at the same time, thus allowing a high degree of control with lessor human effort for large swarms. Most of the HSI frameworks design have been human-centric and focused on direct control of swarms either through teleoperation or

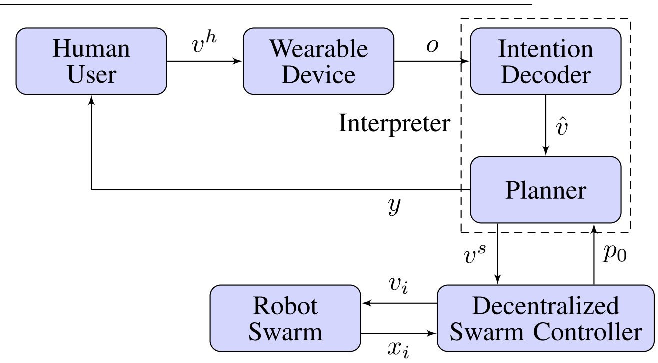


Fig. 1. Workflow of Human Swarm Interface. The user communicates their intent $v^h$ through the wearable. The decoder estimates the user intent $\hat{v}$ from observations $o$. Using this, the planner optimally obtains a set of intermediate goals $v^s$. The decentralized controller present in each agent $i$ reaches $v_i^s$ by computing the velocities $v_i$.

proximal interaction (Jawad et al., 2014; Setter et al., 2015). Due to complicated swarm dynamics, the human will quickly be overwhelmed and would not make the best decisions, as in our previous work (Suresh, 2016; Suresh and Schwager, 2016). Our planner addresses this by generating an intuitive human-approved swarm-friendly plan for the swarm to follow.

More recently, gesture based techniques along with speech, vision and motion have been used together to interact with small teams of robots (Alonso-Mora et al., 2015; Gromov et al., 2016) . These works rely on proximal multi-modal interaction schemes which require complex hardware setup to interpret the human gestures, which is not practical for large scale swarms. We rely on a single wearable device without any other external electronics, which makes the implementation more practical. With respect to formation control for large scale swarms, (Rubenstein et al., 2014) researchers have only used predefined shapes and images as inputs for the swarm, which facilitates only supervisory control for a HSI system. But in

⋆ This work was supported in part by NSF- CMMI 1434819 and AFOSR FA9550-18-1-0158. We are grateful for their support. We thank Mac Schwager for useful discussions regarding the HMM formulation used in this work. We also thank Chidi Ewenike, Ramon Duran and Tomas Torres for their help in developing the Myo armband setup used in this work.

[1] Christensen, H. I., et al. "A roadmap for US robotics: from internet to robotics." (2016). http://jacobsschool.ucsd.edu/contextualrobotics/docs/rm3-final-rs.pdf

2405-8963 © 2019, IFAC (International Federation of Automatic Control) Hosting by Elsevier Ltd. All rights reserved.
Peer review under responsibility of International Federation of Automatic Control.
10.1016/j.ifacol.2019.01.033

our approach the swarm is capable of understanding intuitive human intention with the aid of the interpreter.

*Statement of Contributions.* We propose a novel HSI framework where we consider both a human agent and a dynamic swarm, with an interpreter acting as an bridge between the two. By means of it, the user can communicate their intentions intuitively and naturally, without having an in depth understanding of the swarm dynamics. At the same time, the swarm receives control subgoals in their domain and need not spend resources to decode the user's intention. The paper presents contributions in the following three aspects. On the human-interpreter interaction side, we formulate a novel intention decoder using Kalman Filtering and HMMs for simultaneous dynamic and static gesture decoding utilizing the IMU and EMG sensors, respectively. This method increases intuitiveness as preliminary tests have suggested that the human quickly learns to adapt to this interface, with results being comparable to a standard interfaces like a computer mouse. Second, we further exploit the interpreter element to devise control subgoals that are efficient for the swarm, and which require global information that is not easily accessible for the swarm. In this way, the interpreter solves a planning problem with the goal of controlling the swarm efficiently while following an intuitive behavior. Third, we present a novel discrete second-order distributed formation controller for the swarm that combines the Jacobi Overrelaxation Algorithm and dynamic average consensus to guarantee the convergence of a (second-order integrator) swarm to a desired shape, scaling, rotation and displacement. Our controller relies only on the position information of each agent and communication with their neighbors using variable communication radii, which provides a practical setting. Finally, we highlight a contribution on the integration of diverse tools from control theory, network science, machine learning, signal processing, optimization and robotics that serve to articulate our HSI framework.

## 2. PRELIMINARY CONCEPTS

*Basic Notations.* We let $\mathbb{R}$ denote the space of real numbers, $\mathbb{Z}_{\geq 0}$ the space of positive integers, $\mathbb{R}^n$ and $\mathbb{R}^{M\times n}$ denote the $n$-dimensional real vector space and the space of $MXn$ real matrices, respectively and $\mathbb{P}$ to denote the set of $n$ dimensional polygonal shapes. In what follows, $\mathbf{1}_M \in \mathbb{R}^M$ are column vector of ones, $\mathbf{I} \in \mathbb{R}^{M\times M}$ is the identity matrix, $\mathbf{O} \in \mathbb{R}^{M\times n}$ denotes a matrix of zeros and $\|.\|$ denotes the Euclidean norm. Given a matrix $A \in \mathbb{R}^{M\times M}$, its eigenvalues are denoted by $\{\lambda_1^A, \dots, \lambda_M^A\}$, enumerated by their increasing real parts and its $i^{\text{th}}$ row is denoted by $A_i$.

*Graph Theory Notions.* Consider a swarm of $M$ agents in $\mathbb{R}^n$. Let $p_i(t), v_i(t) \in \mathbb{R}^n$ denote the position and velocity respectively of the $i^{\text{th}}$ agent at time $t$.

We model the communication among agents by means of an undirected $\nu$-disk communication graph $\mathcal{G}_\nu = (V, E_\nu(p))$, where $V = \{1, \dots, M\}$ denotes the set of agents (vertices of the graph), and $E_\nu(p) \subset V \times V$, denotes the set of edges. In particular, $(i,j) \in E_\nu(p)$ if and only if $\|p_i - p_j\| \leq \nu$. The entries of the associated adjacency matrix $A(p) \in \mathbb{R}^{M\times M}$ become:

$$a_{ij} = \begin{cases} 1, & \text{if } \|p_i - p_j\| \leq \nu, \\ 0, & \text{otherwise.} \end{cases}$$

The neighbor set $\mathcal{N}_i$ for the $i^{\text{th}}$ agent is given by $\mathcal{N}_i := \{j \mid a_{ij} = 1\}$. Associated with $\mathcal{G}_\nu$, we consider a weight-balanced weighting $W(t) \in \mathbb{R}^{M\times M}$, where $W(t)$ is the metropolis weight matrix corresponding to the communication graph $\mathcal{G}_\nu$; see (Xiao and Boyd, 2004), and $w_{ij}$ are the corresponding entries of $W$. We let $d_i = A_i(p)\mathbf{1}_M^\top$ be the degree of the $i^{\text{th}}$ agent. We denote by $D \in \mathbb{R}^{M\times M}$ the diagonal degree matrix of $\mathcal{G}$ with $d_i$, the degree of node $i$, being the $i^{\text{th}}$ diagonal entry of $D$. The Laplacian matrix $L \in \mathbb{R}^{M\times M}$ of the graph $\mathcal{G}_\nu$ is given by $L = D - A$, and the normalized laplacian matrix is given by $L^N = D^{\frac{-1}{2}} L D^{\frac{-1}{2}}$ . Similarly the weighted Laplacian matrix is given by $L^W = \mathbf{I} - W$. The connectivity properties of a graph are captured by the second smallest eigenvalue $\lambda_2$ of the Laplacian matrix $L$. We can also express connectivity in terms of $\lambda_2^W$ and $\lambda_2^N$. We can say that the respective graph is connected if $\lambda_2^W, \lambda_2^N > 0$, and connectivity increases with increase in $\lambda_2^W, \lambda_2^N$. Readers can refer (Bullo et al., 2009; Godsil and Royle, 2001) for further details on Graph Theory and its application to robotics.

## 3. PROPOSED FRAMEWORK AND PROBLEM FORMULATION

Here, we first introduce the various timescales involved in the interactions, and propose a new HSI framework, while providing a description of its components. Later, we identify the various problems to be solved to implement this framework.

*Timescales Involved.* We assume that the interactions between the human, interpreter and the swarm, and the dynamic update of the swarm, may occur at time scales that go from coarser to finer resolution. In this way, human and interpreter may interact at discrete times that are a multiple of $\tau_{\text{h}}$, the interpreter and the swarm may interact at multiples of $\tau_{\text{int}} < \tau_{\text{h}}$, while the swarm dynamic update times occur at multiples of $\tau_{\text{s}} < \tau_{\text{int}}$. In what follows, we identify $T \equiv T\tau_{\text{h}} \geq 0$ (resp. $l \equiv l\tau_{\text{int}}$, and $t \equiv l\tau_{\text{s}}$) and we distinguish these integers as belonging to $T \in \mathbb{Z}^{\text{h}}_{\geq 0} \equiv \mathbb{Z}_{\geq 0}$ (resp. $l \in \mathbb{Z}^{\text{int}}_{\geq 0} \equiv \mathbb{Z}_{\geq 0}$, and $t \in \mathbb{Z}^{\text{s}}_{\geq 0} \equiv \mathbb{Z}_{\geq 0}$.) We use the time variable $t$ for the wearable device as it operates at a fast rate, similar to the swarm.

*Proposed Framework.* The user specifies their intentions which are translated by the interpreter and in turn communicated to the swarm. The human uses a wearable device called the MYO armband [2] which observes the human intended swarm command. By means of it, the user specifies a desired formation shape $S \in \mathbb{P}$, centroid $\mathrm{c} \in \mathbb{R}^2$, orientation $\theta \in \mathbb{R}$, and scaling $\mathrm{s} \in \mathbb{R}$ for the swarm. These parameters make up the desired human intention $v$ which the interpreter decodes as $\hat{v}$, where $v, \hat{v} : \mathbb{Z}^{\text{int}}_{\geq 0} \to \mathbb{P} \times \mathbb{R}^2 \times \mathbb{R} \times \mathbb{R}$. The MYO armband receives the human intention $v(T)$ as Electromyography (EMG) signals and Inertial Measurement Unit IMU signals.

The interpreter first uses a decoder (Section 4.1) to translate human intentions $v(T)$ into $\hat{v}(T)$. Then it translates $S(T)$ in $\hat{v}(T)$ to desired relative agent positions $z^f(T) \in \mathbb{R}^{M\times n}$ which best depicts the swarm shape. The swarm also has an operation mode $\mu(t) \in \{1, \dots, m\}$ corresponding to $m$ different communication ranges for each agent of the swarm. We have the notion of swarm operating cost involving $\mu(t)$ as a trade-off between network connectivity and network maintenance costs. We also introduce the notion of Human Interpretable Dynamics (HID), which represents easily understandable swarm dynamics by the Human. Both these concepts will be elucidated in Section 4.4.2.

Now, Given a desired formation $z^f(T)$ and the current state $p(0)$, the interpreter then determines the set of switching intermediate goals $V^s = \{v^s(1), ..., v^s(N)\}$ with $v^s(l) = \{z(l), \mathrm{s}(l), \mathrm{c}(l), \theta(l), \mu(l)\}$, $l \in \{1, \dots, N\}$ and $N$ being the time horizon for switching. These intermediate goals $V^s$ follow the HID and are optimal with respect to the swarm operating costs. These intermediate goals represent way points and intermediate shapes which will be communicated to the swarm. These parameters constitute the high-level commands that the swarm receives and executes via a distributed algorithm. That is, our swarm employs a decentralized control scheme detailed in Section 4.3 to reach $v^s(l)$. Figure 1 illustrates the work-flow of our proposed framework. Thus, from here, we need to solve the following problems to complete our framework:

[2] https://www.myo.com/

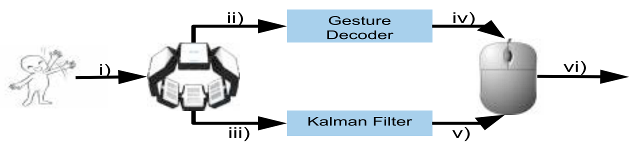


Fig. 2. The user intention decoder system. i) The user conveys their intention through arm movement and gestures. ii) The Myo armband captures the gestures as EMG signals which are read by the gesture decoder. iii) Arm movements are captured as IMU signals and sent to a Kalman filter. iv) The HMM based decoder provides gestures which are mapped to mouse clicks and scrolls. v) The updated state of the Kalman filter is used to assign mouse position. vi) Shape $S$ and centroid c are specified using the GUI (Figure. 4) using iv) and v)

*Problem 1.* (Human Intention Decoder). Given the observations $o$ from the Myo armband, design a decoder to get the desired human intention $\hat{v}(T)$.

*Problem 2.* (Behavior Specifier). Given the desired human intention $\hat{v}$, design an algorithm to produce the goal behavior $V^s$ which can be understood by the swarm.

*Problem 3.* (Planning Algorithm). Given the goal behavior $V^s$, generate the set of optimal intermediate behavior subgoals $\{v^s(l)\}$ with $l \in \{1, \ldots, N\} \cap \mathbb{Z}^{\text{int}}_{\geq 0}$, and $N$ denoting the time horizon, and $N\tau_{\text{int}} \leq T\tau_{\text{h}}$ which follow human-interpretable dynamics and minimize swarm operating costs.

*Problem 4.* (Distributed Swarm Controller). Given the command $v^s(l)$, for some $l \in \mathbb{Z}^{\text{int}}_{\geq 0}$, design a distributed algorithm to drive the swarm to the intermediate shape $z(l)$ with scaling $\mathrm{s}(l)$, rotation $\theta(l)$ and centroid $\mathrm{c}(l)$ using operation mode $\mu(l)$ from some initial position $p(l-1)$.

*Problem 5.* (User Interface Design and Feedback). Develop a Graphical user interface (GUI) for the human to communicate their intention $v$ to the interpreter and receive feedback about the decoded intention $\hat{v}$ and the state of the swarm.

## 4. TECHNICAL APPROACH

The solutions to the above problems are briefly explained here, the reader can refer the extended version (Suresh and Martínez, 2018) for detailed explanations and proofs.

### *4.1 Problem 1: Intention Decoding*

The user conveys their intention $v$ through gestures and arm movement which are recorded by the Myo armband as EMG signals. The intention decoder deciphers discrete arm gestures and arm position using the EMG and IMU sensors respectively. The gestures and arm movement are translated to mouse clicks and mouse movements according to Figure 3, which provide feedback of the decoded intended gesture $\hat{v}(T)$ to the user. The entire pipeline is described in Figure 2.

### *4.2 Problem 5: User Interface Design*

We developed a GUI in MATLAB which takes in the input a computer mouse and performs the desired behavior with simulated robots. The user interacts with the GUI using arm movements and gestures which are mapped to mouse movements and mouse clicks according to Section 4.1 and Figure 2. Figure 4 illustrates a snapshot of the GUI during the planning phase which has 5 different zones, whose selection will be triggered by hovering over to the desired area with the mouse pointer. For more details please refer to the extended version (Suresh and Martínez, 2018)

### *4.3 Problem 4: Swarm Controller*

Our swarm controller is designed to achieve the interpreter's intention $v^s(l) := \{z(l), \mathrm{s}(l), \mathrm{c}(l), \theta(l), \mu(l)\}$ at time $l\tau_{\text{int}}$.

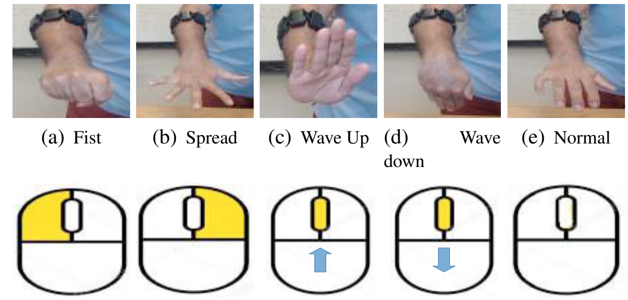

(a) Fist (b) Spread (c) Wave Up (d) Wave down (e) Normal

(f) Left click (g) Right click (h) Scroll up (i) Scroll down (j) Normal

Fig. 3. (a)-(e) show the various gestures used and (f)-(j) indicate the corresponding mouse functionalities.

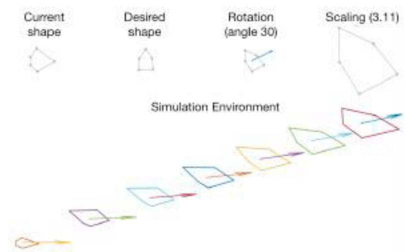


Fig. 4. UI used to interact with the interpreter.

Having second-order integrator dynamics for the agents, and the need of controlling the swarm centroid motivates our controller which extends (Cortés, 2009) (for first-order agents) with the dynamic consensus feedback interconnection of (Zhu and Martínez, 2010).

With $p_i, v_i$ being the position and velocity of the $i^{\text{th}}$ agent, our second-order distributed swarm controller takes the form:

$$
\begin{aligned}
p_i(t+1) =& p_i(t) + v_i(t), \qquad\qquad (1a)\\
v_i(t+1) =& -\alpha(p_i(t) + v_i(t)) + \\
& \frac{\alpha}{d_i(t)} \sum_{j \neq i} \{a_{ij}(t)(p_j(t) + v_i(t)) + \\
& \mathrm{s}(l) d_i(t)(z_i(l) - z_j(l)) R^{\theta}(t)\} - k^p(c_i(t+1) - \mathrm{c}(l)),\\
c_i(t+1) =& c_i(t) + \\
& \sum_{j \neq i} w_{ij}(c_j(t) - c_i(t)) + p_i(t) - p_i(t-1), \qquad (1b)
\end{aligned}
$$

where $k^p, \alpha \in (0,1)$ are control gains and $R^{\theta}$ is the rotation matrix corresponding to $\theta$. The variable $c_i(t) \in \mathbb{R}^n$ is the estimated center of the swarm by the $i^{\text{th}}$ agent. Note that the $w_{ij}$ are the Metropolis weights defined in Section 2. This algorithm, which applies to second-order systems, cancels out the drift observed in (Cortés, 2009) with the help of dynamic consensus, and drives the swarm to the desired centroid at time $l\tau_{\text{int}}$. The FODAC algorithm in (Zhu and Martínez, 2010) in equation (1b) is used to distributively estimate the mean of time varying reference signal $p(t)$ which would give us the estimate of the swarm's centroid $c(t)$.

It is interesting to note that the swarm controller (1) consists of autonomous components and a controlled component which house the desired interpreter's intention $v^s(l)$. So $v^s(l)$ can be communicated once at the beginning of the $l^{\text{th}}$ iteration and the agents just need to adjust their positions and communicate locally with their neighbors to achieve the intermediate goal.

We will make use of the following assumptions on $\mathcal{G}_{\mu}(t)$ to analyze this controller:

*Assumption 1.* (Connectivity). The communication graph $\mathcal{G}_{\mu}(t)$ has at least one globally reachable vertex at every time $t$.

*Assumption 2.* (Constant graphs). The communication graph $\mathcal{G}_\mu(t)$ remains constant for $t \in [(l-1)\tau_{\text{int}}, l\tau_{\text{int}}]$.

With $\delta_1 = 1-(1-\alpha\lambda_2^N)^2$, $\delta_2 = 1-(1-\lambda_2^W)^2$ we can state the following theorem:

*Theorem 1.* (Stability of Swarm Controller). Under Assumption 1 (connectivity) and Assumption 2 (constant interconnection graph), with the control gains satisfying $k^p < \frac{\delta_1\delta_2}{2}$, the swarm globally uniformly asymptotically stabilizes to the desired state $X_d$ under the swarm controller dynamics (1) from any initial condition.

We will use the results of Theorem 1 to get an intuition of the role of graph connectivity ($\lambda_2^N$ and $\lambda_2^W$) in the convergence of our swarm controller (1).

*Corollary 1.* The convergence rate of (1) is directly proportional to $\lambda_2^N$ and $\lambda_2^W$ of the communication graph.

The proof of Corollary 1 and Theorem 1 is presented in the Appendix of the extended version (Suresh and Martínez, 2018). Using these results we will design a planning algorithm, which optimally determines the intermediate subgoals which will be described in Section 4.4.2.

### 4.4 The Interpreter

For ease of illustration, we consider the formulation in 2D space. The interpreter mainly consists of two parts: the behavior specifier and the planner.

*Problem 2: Behavior Specifier* The Behavior specifier converts the desired human intention into parameters that can be comprehended by the swarm. The human user specifies the desired shape $S^d \in \mathbb{P}$ which takes the form of an arbitrary polygon, the desired centroid $\mathrm{c}^d \in \mathbb{R}^2$, scaling $\mathrm{s}^d \in \mathbb{R}$ and rotation $\theta^d \in \mathbb{R}$. The interpreter then decides the formation denoted by the relative positions of the agent $z^d \in \mathbb{R}^{M\times n}$, which would best illustrate the shape $S^d$ given by the human. For simplicity, we use a uniform distribution in the interior of the shape $S^d$ to obtain $z^d$, which is illustrated in Figure 5(b). For more explanation please refer to the extended version of the draft (Suresh and Martínez, 2018). The parameters $z^d$, $S^d$, $\mathrm{c}^d$, $\mathrm{s}^d$ and $\theta^d$ are passed on to the planner.

*Problem 3: Planner* The Planner uses the received decoded human intention parameters to construct a set of intermediate way points $\{S(l), \mathrm{s}(l), \theta(l), \mathrm{c}(l)\}$, $\forall l \in \{1,\dots,N\}$, where $N$ denotes the number of intermediate steps in the plan to reach the final goal.

To do this, we employ an $N$-Horizon Discrete Switched Linear Quadratic Regulator (DSLQR) formulation. A particular DSLQR problem with a dynamical variable $h \in \mathbb{R}^d$ and time horizon $l \in \{1,\dots,N\}$ can be formulated as follows:

$$\min J(u,\mu) = \sum_{l=0}^{N}(h(l)^\top Q_\mu h(l) + u(l)^\top R_\mu u(l)) + h(N)^\top Q_f h(N), \quad (2a)$$

$$\text{subject to } h(l+1) = \mathcal{A}h(l) + \mathcal{B}u(l), \quad (2b)$$

where $h(0) = h_0$. Here, the running cost consist of a switching LQ cost function, with parameterized matrices $Q_\mu$ and $R_\mu$, depending on a mode $\mu$. The function will be designed to enhance swarm performance while the linear constraint will be used to enforce an easy-to-interpret behavior by a human, which defines a Human Interpretable (HID) dynamics.

Details and methodology of DSLQR systems can be found in (Zhang et al., 2009). We show next how we apply this approach in our particular setup and describe the matrices that we choose for our framework.

(i) *Human-Interpretable Dynamics:* We introduce the notion of Human Interpretable Dynamics (HID) to denote a dynamical system that can be easily understood by a human. Since the interpreter needs to provide feedback to the user, the planner needs to provide an abstraction of the complicated swarm dynamics in an $Mn$-dimensional space. These dynamics need to be slower than the swarm dynamics to enhance human interpretability, and are hence implemented in the $l$ timescale described in Section 3.

(a) HID illustration (b) Formation Specifier

Fig. 5. (a) HID illustration for shape changing from rotated cone to a standing rectangle. The model parametrs used are $\mathcal{A} = \mathcal{B} = Q = \mathbf{I}_h$, $R = 100\mathbf{I}_h$ and $Q_f = 1500\mathbf{I}_h$. (b) Left: The user specifies the desired shape $S^d$ by providing $v$ vertices (triangles). Right: the interpreter determines the relative positions $z^d$ of $M = 500$ agents (blue dots) to represent the shape drawn by user.

Here, we propose a simple linear dynamical system approach to model these dynamics, which takes into account the desired human intention $h^d = (S^d, \mathrm{s}^d, \theta^d, \mathrm{c})$. We suppose that fully actuated linear dynamical systems are more easily understandable by humans, as opposed to other nonlinear system models. We let $h = [S, \mathrm{s}, \theta, \mathrm{c}]^\top$ denote the state of the HID system with $h(l) \in \mathbb{H}$, where $\mathbb{H} = \mathbb{P}\times\mathbb{R}^n\times\mathbb{R}\times\mathbb{R}$. Then, the HID takes the form:

$$h(l+1) = \mathcal{A}h(l) + \mathcal{B}u(l), \quad (3)$$

where matrices $\mathcal{A}, \mathcal{B} \in \mathbb{H}\times\mathbb{H}$ and control input $u \in \mathbb{H}$. In this paper, we choose $\mathcal{A}$ and $\mathcal{B}$ to be identity matrices. This seems to be the most intuitive dynamics as the control input applies directly on the system. In future work, we will study alternative choices for these dynamics and conduct human studies to validate our proposition.

We use the $N$ horizon Discrete LQR control technique to drive the HID towards $h^d$ starting from some initial configuration $h(0) = h_0$. By considering a change of variable $h^e(l) = h(l) - h^d$, we define a first term contributing to the problem cost functional as follows:

$$J_{\text{HID}}(u) = \sum_{l=0}^{N-1}(h^{e\top}(l) Q h^e(l) + u(l)^\top R u(l)) + h^e(N)^\top Q_f h^e(N). \quad (4)$$

where the matrices $Q, R, Q_f \in \mathbb{H}\times\mathbb{H}$ are positive definite and $u(l)$, $\forall l \in \{1,\dots,N\}$ is a step change applied during the $l^{\text{th}}$ time. So $u(l)$ is chosen such that the cost $J_{\text{HID}}$ is minimized. This is solved using the standard LQR approach, and the results are shown in Figure 5(a) for a $N = 10$ horizon problem. Figure 5(a) shows the stages of transformation of a 5 sided polygon to a rotated and translated 4 sided polygon. The figure depicts a seemingly natural transition which can be easily interpreted by the user, thus justifying the HID formulation. The case of mismatch in the number of vertices in the initial and desired shapes is handled by adding vertices appropriately on the perimeter of the shape that has fewer vertices.

(ii) *Swarm Performance Costs.* We just discussed how to generate intermediate shapes taking into account the HID. Now we consider the swarm performance and communication cost to choose the operating mode $\nu$ in the general setup. The operating modes $\nu$ correspond to a subset of $\nu$-disk graphs defined over the swarm when distributed over a shape. Since agent formations are chosen in a consistent manner as described in e.g. Figure 5(b), the number of possible graphs over the agents for different $\nu$ is very much reduced and remains constant for scaled shapes. From now on, we consider this set is given by $\{\nu_1, \ldots, \nu_m\}$ by choosing appropriate communication radii.

*Operating costs involved:* To increase the speed of convergence and to facilitate quicker interpretation by a human, we need to maximize the notion of connectivity involving the second smallest eigenvalue $\lambda_2^N$ or $\lambda_2^W$ of the respective Laplacian matrices $L^N$ and $L^W$. This can be found from the determinant of the matrix $G \in \mathbb{R}^{(M-1)\times(M-1)}$ defined as $G = F^\top L^N F$ with $F \in \mathbb{R}^{M\times(M-1)}$, $F\mathbf{1}_M = 0$ and $F^\top F = \mathbf{I}$. Since the determinant of a matrix is a product of its eigenvalues, connectivity determined by $\lambda_2^N$ increases iff the determinant of $G$ increases. So the connectivity cost $J_{\text{CON}}(l)$ being in formation $z$ and operation mode $\nu$ at time $l$ is given by:

$$J_{\text{CON}}(\nu, h) = -\kappa_1 \log\det(\kappa_2 G_\nu(l)). \quad (5)$$

To ensure $J_{\text{CON}}$ remains well scaled and positive we introduce positive constants $\kappa_1$ and $\kappa_2$ respectively. Having $\nu$ corresponding to a higher communication radius implies that we will be using more energy to communicate and maintain communication links. This is encoded as a communication cost $J_{com}(l)$ given by

$$J_{\text{COM}}(\nu, h) = \kappa_3 \log(\nu_\nu^2 \mathbf{1}_M^\top A_\nu(h)\mathbf{1}_M), \quad (6)$$

where $\nu(l)$ is the communication range at time $l$ and $\kappa_3$ is a positive constant used for scaling.

Adding these costs (4),(5),(6) together defines the total cost used by the planner as:

$$J(u,\nu) = \sum_{l=0}^{N-1} (\bar{h}^e(l)^\top \overline{Q}_{\nu(l)} \bar{h}^e(l) + \overline{u}(l)^\top \overline{R}\overline{u}(l) + \bar{h}^e(N)^\top Q_f \bar{h}^e(N). \quad (7)$$

where $\overline{Q}_\nu = \begin{bmatrix} Q & 0 \\ 0 & J_{\text{CON}}(\nu) + J_{\text{COM}}(\nu) \end{bmatrix}$, $\bar{h}^e = \begin{bmatrix} h^e \\ 1 \end{bmatrix}$, $\overline{u} = \begin{bmatrix} u \\ 0 \end{bmatrix}$ and $\overline{R} = \begin{bmatrix} R & 0 \\ 0 & 1 \end{bmatrix}$. Observe that a solution to the above problem requires the evaluation of all possible graph combinations for different chosen controls $u$. By choosing the graphs based on the communication radii, and considering a class of formations, we reduce significantly the number of possible graphs to evaluate. In addition, we employ the DSLQR formulation from (Zhang et al., 2009) to obtain the optimal set of $u(l)$ and $\nu(l)$ which minimizes $J$. Our optimization is done in the following sequential manner: first we optimize in the sequence of $\bar{h}^e$ and $\overline{u}$, then, given this, we optimize in the $\nu$ variable using the DSLQR approach from (Zhang et al., 2009). This is further illustrated and discussed in Section 5.3.

## 5. IMPLEMENTATION RESULTS

### 5.1 System Setup

The user has the choice to use either the MYO armband or the mouse to interact with a GUI to control the formation of a simulated swarm in a two dimensional environment. The swarm controller developed in Section 4.3 essentially generates waypoints for the swarm to follow, we assume holonomic dynamics for the individual agents and assume they reach their respective waypoints. We do not focus on collision avoidance, which will be addressed in future work. We utilize the ROS kinetic framework with Python scripting language to interface with the MYO armband and control the mouse pointer. We use Matlab to create the GUI shown in Figure 4, which uses the mouse or the MYO armband as an input device. For the formation controller we set the control gain $\alpha = 0.15$ and proportional constant $k^p = 0.03$.

### 5.2 Intention Decoding

We performed tests to gauge the accuracy and speed of the proposed HMM and Kalman Filter models. For the HMM model, some of our previous tests had given an accuracy levels of over 90% on an average (Suresh, 2016) for similar gestures and framework. On preliminary tests we observed similar results and hence, in the interest of space, we skip this accuracy test for the HMM model. For the effectiveness of the arm movement decoder, we compare the results of operating a mouse with and without the MYO armband. Figure 6 represents the aggregate results over 5 trials. The user was tasked to continuously trace a pentagon which represents the human intention for a minute. It can be seen from the Figure 6 that the results are similar for both cases. Table 1 describes the error involved in each of the trials. It can be seen that the errors involved are about the same with both interfaces, however the speed of using the mouse is higher than the other. This is also due to the fact that users are accustomed to using the mouse for years and need time to adapt to the new interface. But in the 5th trial it can be seen that the performance with the wearable matches many trials with the mouse, which shows that the user can adapt quickly to use the new interface.

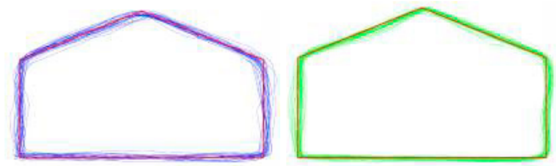

(a) Mouse movement with wearable (b) Mouse movement without wearable

Fig. 6. Aggregate results of tracing a pentagon.(Red) a) The user specifies the shape by using MYO armband. (Blue) b) The user specifies the shape by using the mouse. (Green)

Table 1. Error comparison mouse and wearable.

| | Mouse | | | Wearable | | |
|---|---|---|---|---|---|---|
| Sl. no | Loops | Avg Error | Total Error | Loops | Avg Error | Total Error |
| 1 | 7 | 0.026 | 122.57 | 5 | 0.038 | 179.26 |
| 2 | 8 | 0.028 | 129.40 | 5 | 0.037 | 174.74 |
| 3 | 9 | 0.031 | 147.02 | 7 | 0.048 | 222.07 |
| 4 | 8 | 0.031 | 148.92 | 7 | 0.05 | 235.27 |
| 5 | 9 | 0.035 | 161.50 | 5 | 0.029 | 132.72 |

### 5.3 DSLQR Formulation

The intention decoder can be used for a wider and more intuitive range of applications apart from connecting it to the computer mouse which will be explored in future work. Now we will validate the proposed framework by running simulations of a swarm of 50 agents to reach the desired human intention. Below, we illustrate a particular execution of our framework.

Figure 7(a)-(d) indicate the desired human intention communicated by the human. Using $\mathcal{A} = \mathcal{B} = Q = \mathbf{I}_h$, $R = 100\mathbf{I}_h$, $Q_f = 1500\mathbf{I}_h$, $\kappa_1 = 10^6$, $\kappa_2 = 0.05$, $\kappa_3 = 2 \times 10^4$ the planner was implemented for a $N = 8$ horizon problem with $m = 3$ subsystems. The communication ranges are $\nu(l) \in \{10, 40, 150\}$, corresponding to the three operating modes. Figure 7(e) illustrates the intermediate shapes resulting from the 8 horizon planner, starting from the current intention(triangle on the left), to the desired intention(larger rotated quadrilateral) on the right. The intermediate shapes look natural and the progression is gradual and intuitive, which justifies the notion of HID. Figure 7(f) describes the evolution of the cost from equation (7) and switching strategy in a backward horizon. We can see that switching occurs in a timely manner to maintain minimum costs according to equation (7). Switching occurs from 1st mode to the 2nd mode during the 2nd timestep. During the 7th timestep another switching occurs to the 3rd operating mode to maintain minimum cost. This is coherent with the intuition of using larger communication radii for more sparse swarms. As the scaling increases with every timestep the agents are forced further apart and the cost of using a smaller com-


(a) Current shape

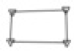
(b) Desired Shape

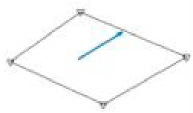
(c) Desired rotation: $\theta^d = 50°$

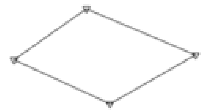
(d) Desired scaling: $s^d = 11.6$


(e) Planning and Execution

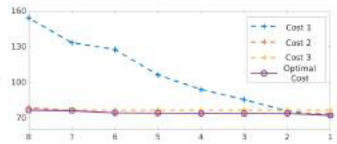

(f) Switching cost throughout execution

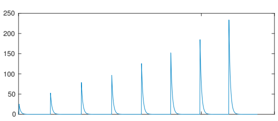
(g) Formation error $e^f(t)$

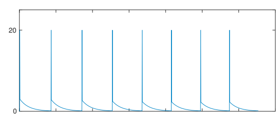
(h) Centroid error $e^c(t)$

Fig. 7. Results of executing a particular desired behavior communicated by the human.

munication range $\nu = 10$ rapidly increases. Whereas, the cost of using the largest range $\nu = 150$ remains almost constant throughout because the connectivity and communication costs mostly remain the same. Figure 7(e) shows the execution of the swarm controller during the $l = 2$ horizon. Each of the red dots represent individual agents of the swarm. We evaluate the performance of the swarm controller (1) by measuring the error with respect to the intermediate formations and centroid at each time step $t$. The formation error and centroid error are measured as $e^f_l(t) = \|p(t) - s(l)z(l)R(\theta(l))\|$ and $e^c_l(t) = \|c(t) - c^d(l)\|$ respectively in reaching the $l^{\text{th}}$ intermediate goal. The evolution of these errors(y-axis) with respect to time $t$(x-axis) is illustrated in Figures 7(g) and 7(h). We see that the swarm successfully reaches every intermediate goal and finally reaches the desired human intention.

## 6. CONCLUSIONS AND FUTURE WORK

In this work we have proposed and successfully implemented a novel HSI framework for formation control, where the user draws the desired shape using intuitive gestures, and the swarm successfully depicts the drawn shape. We have combined diverse tools from control theory, network science, machine learning, signal processing, optimization and robotics to create this multi-disciplinary framework. Firstly, we have demonstrated the effectiveness and intuitiveness of human interaction using this framework, whose accuracy and speeds are comparable to standard interaction devices. Next, we have proposed and utilized a unique notion of human interpretable dynamics along with switching systems to plan intermediate natural shapes for the swarm to depict, which can be easily understood by the human and the swarm. We have also developed, analyzed and illustrated a novel decentralized formation controller capable of reaching any shape and centroid in the 2-D space. Lastly, we have integrated the framework by developing a GUI environment which interacts with user by means of gestures, and rest of the framework is encapsulated in the GUI using matlab simulations.

Future work will involve validation of the proposed framework with robustness towards noise and uncertainties. We also wish to learn the Human Interpret-able dynamics from existing human behavior models and data.

## REFERENCES

Alonso-Mora, J., Lohaus, S., Leemann, P., Siegwart, R., and Beardsley, P. (2015). Gesture based human - Multi-robot swarm interaction and its application to an interactive display. In *IEEE Int. Conf. on Robotics and Automation*, 5948–5953.

Bullo, F., Cortés, J., and Martínez, S. (2009). *Distributed Control of Robotic Networks*. Applied Mathematics Series. Princeton University Press.

Cortés, J. (2009). Global formation-shape stabilization of relative sensing networks. In *American Control Conference*, 1460–1465. St. Louis, MO.

Franchi, A. (2017). *Human-Collaborative Schemes in the Motion Control of Single and Multiple Mobile Robots*, 301–324. Springer International Publishing.

Franchi, A., Secchi, C., Ryll, M., Bulthoff, H.H., and Giordano, P.R. (2012). Shared control: Balancing autonomy and human assistance with a group of quadrotor uavs. *IEEE Robotics and Automation Magazine, Special Issue on Aerial Robotics and the Quadrotor Platform*, 19, 57–68.

Godsil, C.D. and Royle, G.F. (2001). *Algebraic Graph Theory*, volume 207 of *Graduate Texts in Mathematics*. Springer, New York.

Gromov, B., Gambardella, L., and Di Caro, G. (2016). Wearable multi-modal interface for human multi-robot interaction. In *IEEE Int. Symposium on Safety, Security, and Rescue Robotics*, 240–245.

Jadbabaie, A., Lin, J., and Morse, A.S. (2003). Coordination of groups of mobile autonomous agents using nearest neighbor rules. *IEEE Transactions on Automatic Control*, 48(6), 988–1001.

Jawad, N., Giusti, A., Gambardella, L., and Di Caro, G. (2014). Human-swarm interaction using spatial gestures. In *IEEE/RSJ Int. Conf. on Intelligent Robots & Systems*, 3834–3841.

Kolling, A., Phillip, W., Chakraborty, N., Sycara, K., and Lewis, M. (2016). Human Interaction with Robot Swarms: A Survey. *IEEE Transactions on Human-Machine Systems*, 46(1), 9–26.

Olfati-Saber, R., Fax, J.A., and Murray, R.M. (2006). Consensus and cooperation in multi-agent networked systems. *Proceedings of the IEEE*, 95(1), 215–233.

Rubenstein, M., Cornejo, A., and Nagpal, R. (2014). Programmable self-assembly in a thousand-robot swarm. *Science*, 345.

Savla, K. and Frazzoli, E. (2012). A dynamical queue approach to intelligent task management for human operators. *Proceedings of the IEEE*, 19, 672–686.

Setter, T., Fouraker, A., Kawashima, H., and Egerstedt, M. (2015). Haptic interactions with multi-robot swarms using manipulability. *Journal of Human-Robot Interaction*, 4(1), 78–95.

Suresh, A. (2016). *Body swarm interface (BOSI): controlling robotic swarms using human bio-signals*. Master's thesis, Boston University.

Suresh, A. and Martínez, S. (2018). Gesture based human-swarm interactions for formation control using interpreters. *arXiv preprint arXiv:1804.08676*.

Suresh, A. and Schwager, M. (2016). Brain-Swarm Interface (BSI): Controlling a Swarm of Robots with Brain and Eye Signals from an EEG Headset. *arXiv preprint arXiv:1612.08126v1*.

Wang, Z. and Schwager, M. (2016). Kinematic multi-robot manipulation with no communication using force feedback. In *IEEE Int. Conf. on Robotics and Automation*, 427–432. doi:https://doi.org/10.1109/icra.2016.7487163.

Xiao, L. and Boyd, S. (2004). Fast linear iterations for distributed averaging. *Systems and Control Letters*, 53, 65–78.

Zhang, W., Hu, J., and Abate, A. (2009). On the value functions of the discrete-time switched lqr problem. *IEEE Transactions on Automatic Control*, 54(11), 2669–2674.

Zhu, M. and Martínez, S. (2010). Discrete-time dynamic average consensus. *Automatica*, 46(2), 322–329.